

Water Resources Research

Supporting Information For

Intensification of global hydrological droughts under anthropogenic climate warming

**Lei Gu¹, Jiabo Yin^{2*}, Louise J. Slater³, Jie Chen^{2*}, Hong Xuan Do⁴, Hui-Min Wang⁵, Lu
Chen¹, Zhiqiang Jiang¹, Tongtiegang Zhao⁶**

¹School of Civil and Hydraulic Engineering, Huazhong University of Science and Technology, Wuhan, 500074, China

²State Key Laboratory of Water Resources and Hydropower Engineering Science, Wuhan University, Wuhan, 500072, China

³School of Geography and the Environment, University of Oxford, Oxford, UK

⁴Faculty of Environment and Natural Resources, Nong Lam University, Ho Chi Minh City, Vietnam

⁵Department of Civil and Environmental Engineering, National University of Singapore, Singapore

⁶Center of Water Resources and Environment, Southern Marine Science and Engineering Guangdong Laboratory (Zhuhai), School of Civil Engineering, Sun Yat-Sen University, Guangzhou, 510275, China

*Correspondence: Jiabo Yin (jboyn@whu.edu.cn), Jie Chen (jiechen@whu.edu.cn)

Contents of this file

Figures S1 to S23

Introduction

This document provides 23 supplementary figures, which are referred to in the main text as Figure S1-S23.

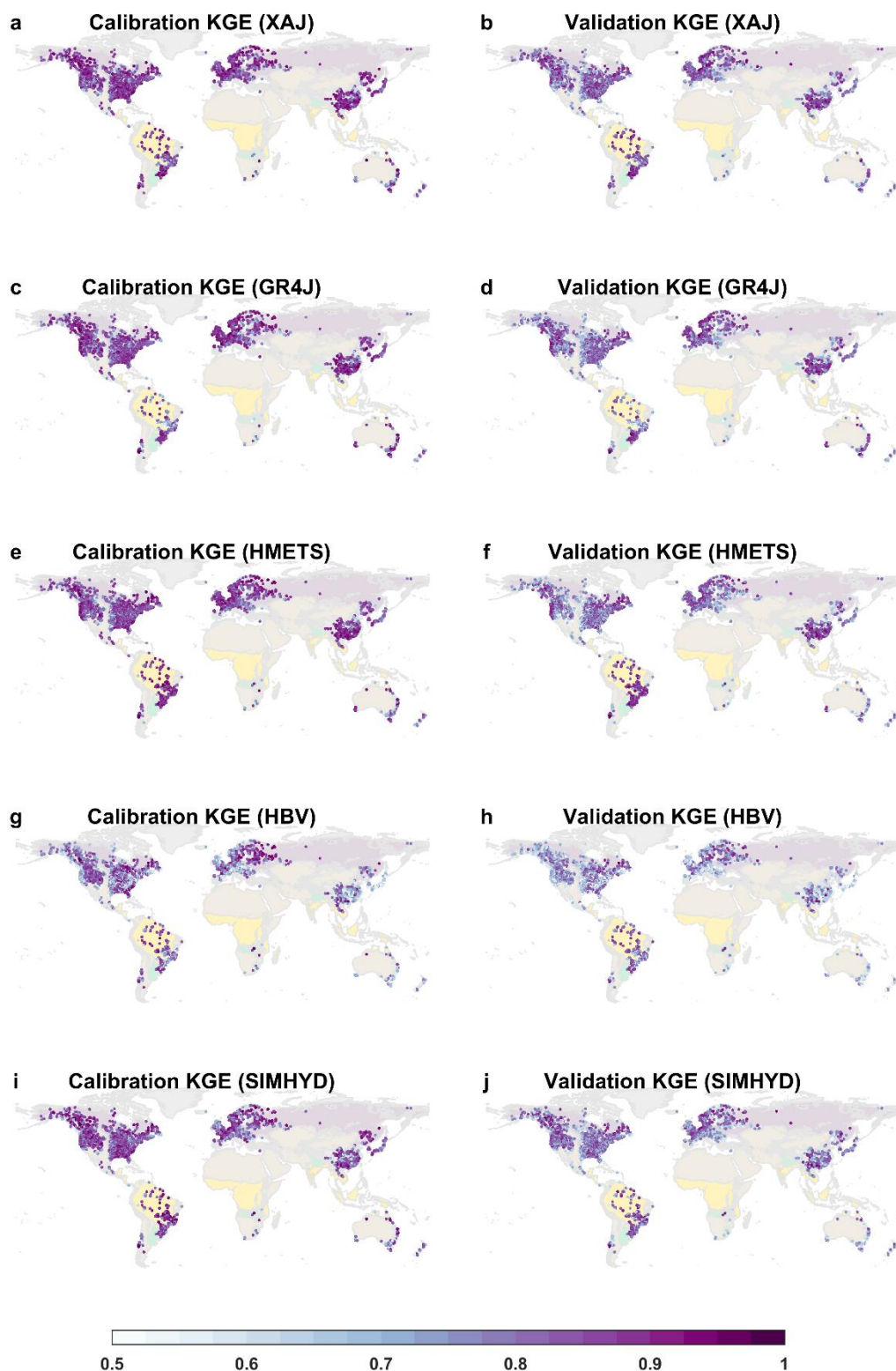


Figure S1 KGE metric for five hydrological models in the calibration and validation periods, respectively. a-b, KGE for XAJ model. c-d, KGE for GR4J model. e-f, KGE for HMETs model. g-h, KGE for HBV model. i-j, KGE for SIMHYD model.

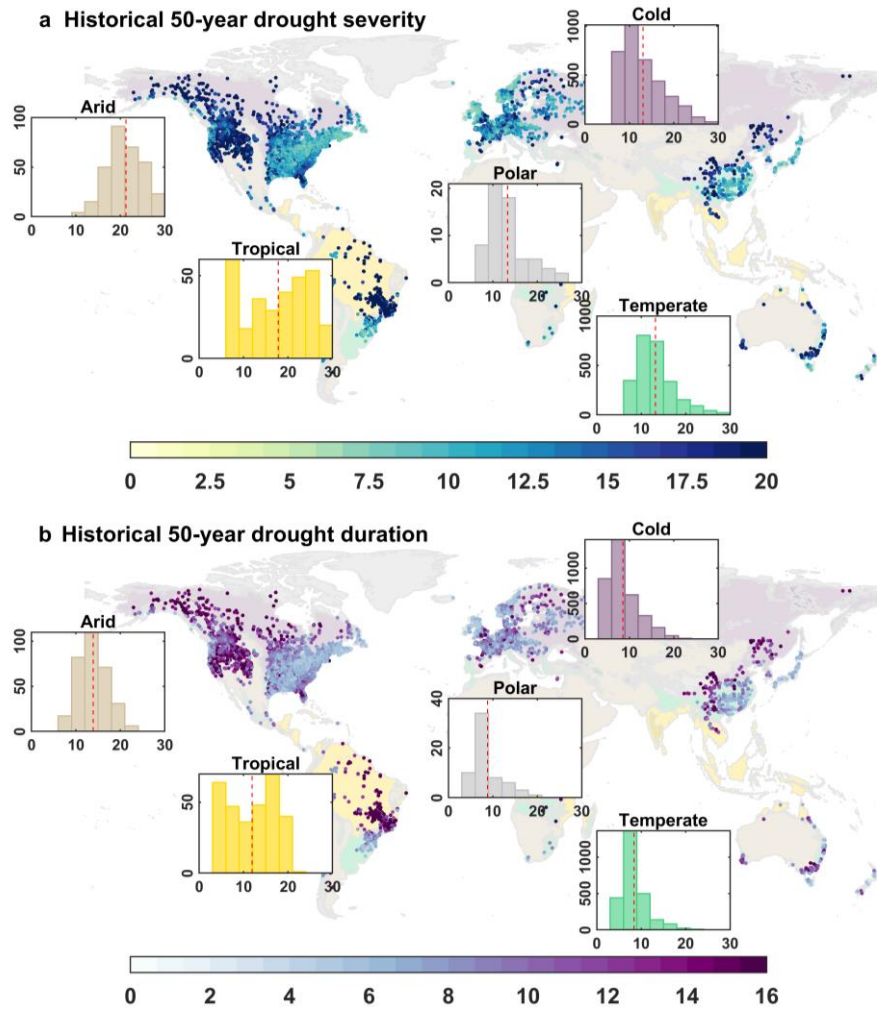


Figure S2 Historical 50-year hydrological drought severity and duration in five climate zones. The scatter shows drought severity (a) and duration (b) from MMM results during the historical 1985-2014 period. The five inserted histograms demonstrate drought severity (a) and duration (b) for catchments inside each climate zone (Arid, Tropical, Polar, Cold, and Temperate). The x-axis denotes drought severity (a) and duration (b) while the y-axis denotes the counts of catchments in each climate zone.

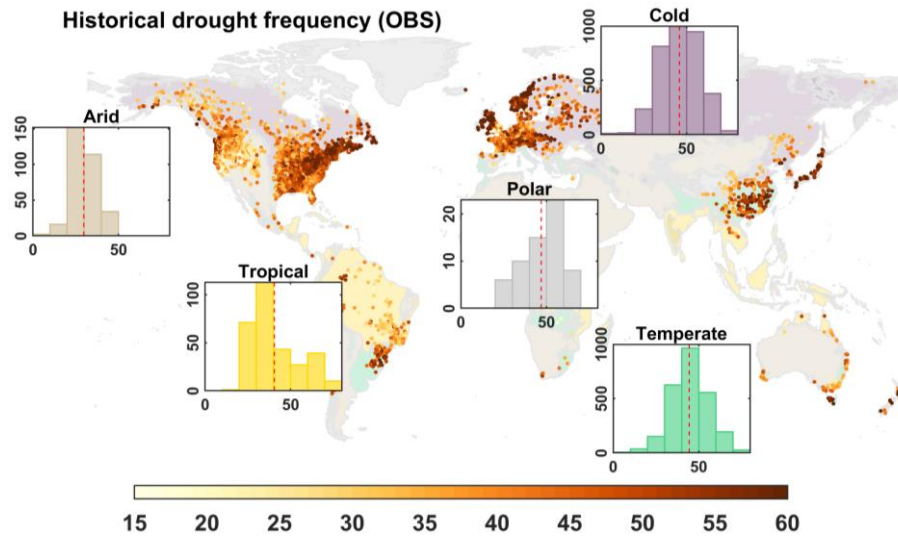


Figure S3 Historical hydrological drought occurrence in five climate zones. The background color shows five climate zones using the Köppen-Geiger climate classification and the colored circles shows drought frequency from observed streamflow (here streamflow denotes time series driven by hydrological models using observed climate data) during the historical 1985-2014 period. The five inserted histograms demonstrate drought frequency for catchments inside each climate zone (Arid, Tropical, Polar, Cold, and Temperate). The x-axis denotes drought frequency while the y-axis denotes the counts of catchments in each climate zone.

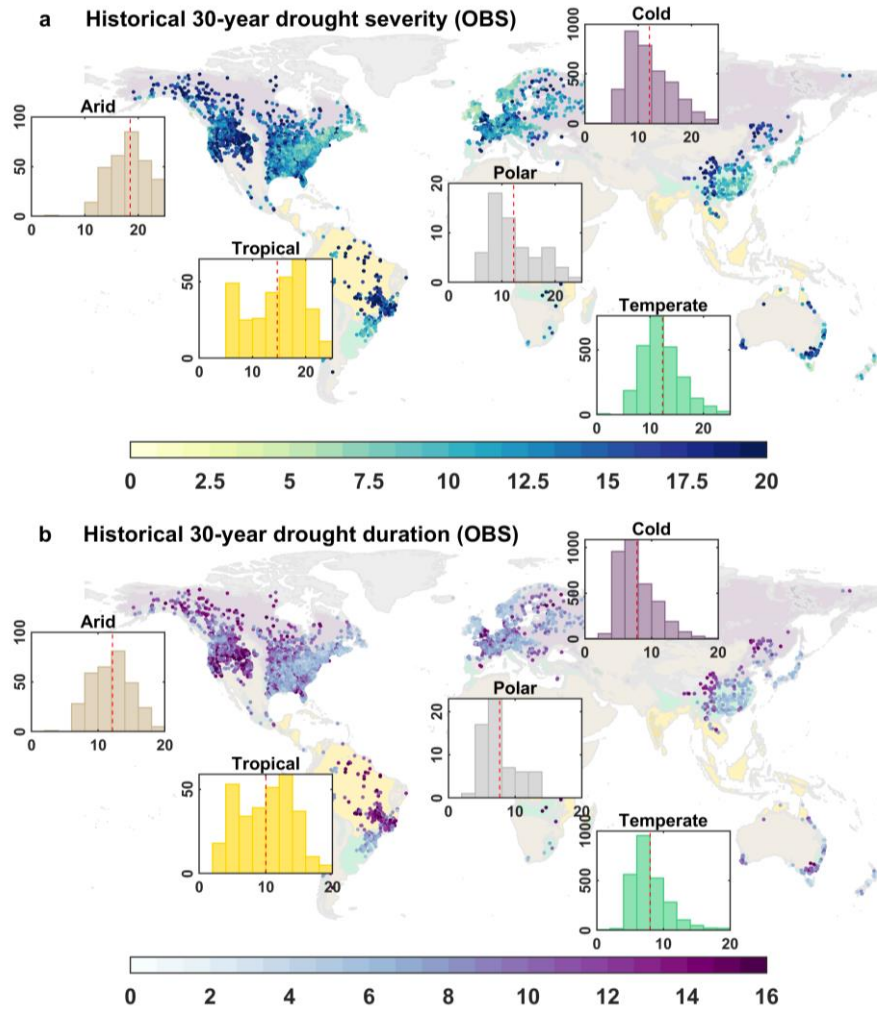


Figure S4 Historical 30-year hydrological drought severity and duration in the five climate zones. The background color shows five climate zones using the Köppen-Geiger climate classification and the colored circles shows drought severity (a) and duration (b) from observed streamflow (here streamflow denotes time series driven by hydrological models using observed climate data) during the historical 1985-2014 period. The five inserted histograms demonstrate drought severity (a) and duration (b) for catchments inside each climate zone (Arid, Tropical, Polar, Cold, and Temperate). The x-axis denotes drought severity (a) and duration (b) while the y-axis denotes the counts of catchments in each climate zone.

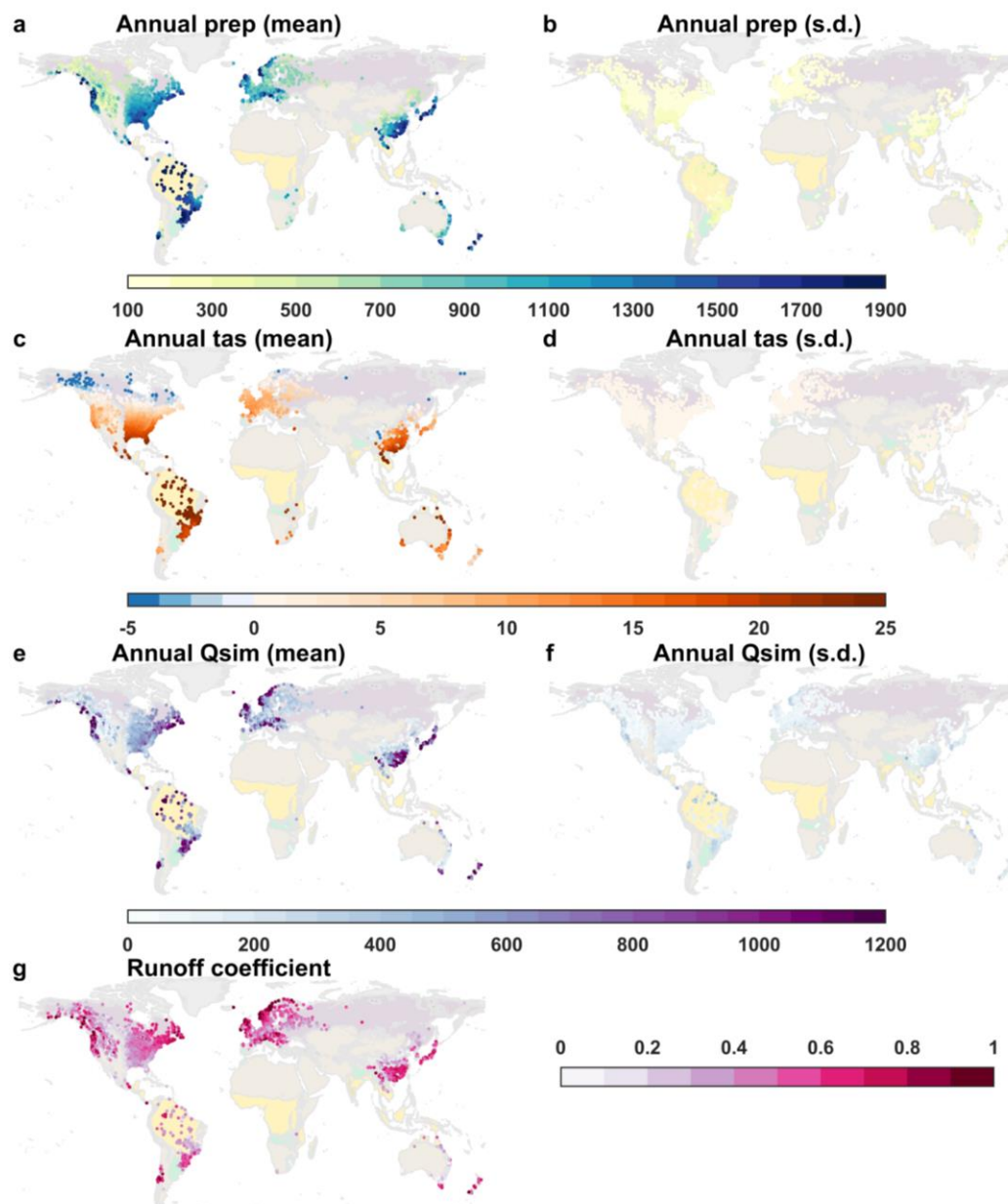


Figure S5 Annual precipitation (prep, mm), temperature (tas, °C), runoff (Qsim, mm) and runoff coefficients during the historical 1985-2014 period.

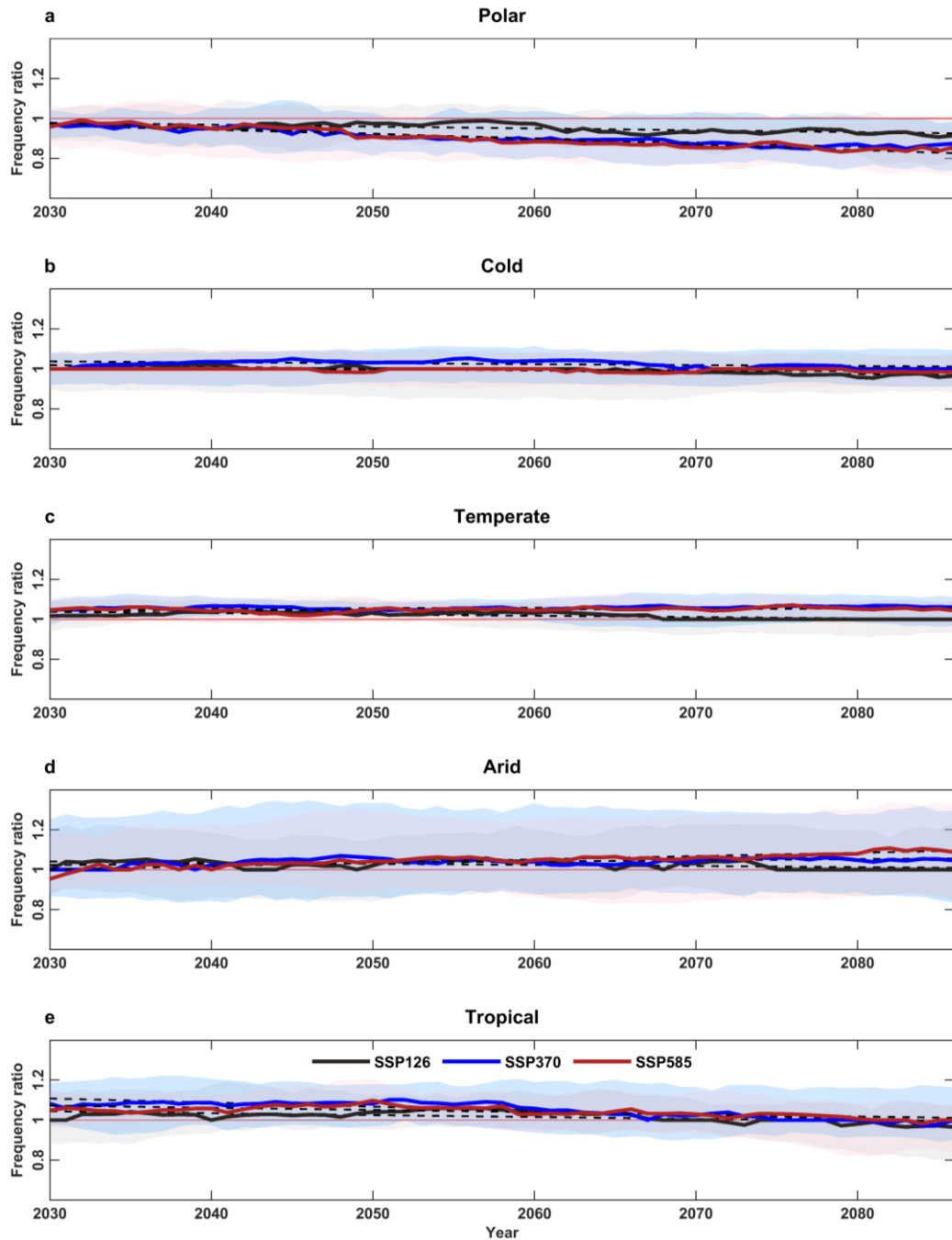


Figure S6 Projected trends and associated uncertainty in hydrological drought frequency ratios in the five climate zones. The colored shaded area represents the uncertainty across models (five global climate models multiply by five hydrological models) and the black (colored dashed) line represents the linear trend line (spatially-averaged frequency ratios) for hydrological droughts.

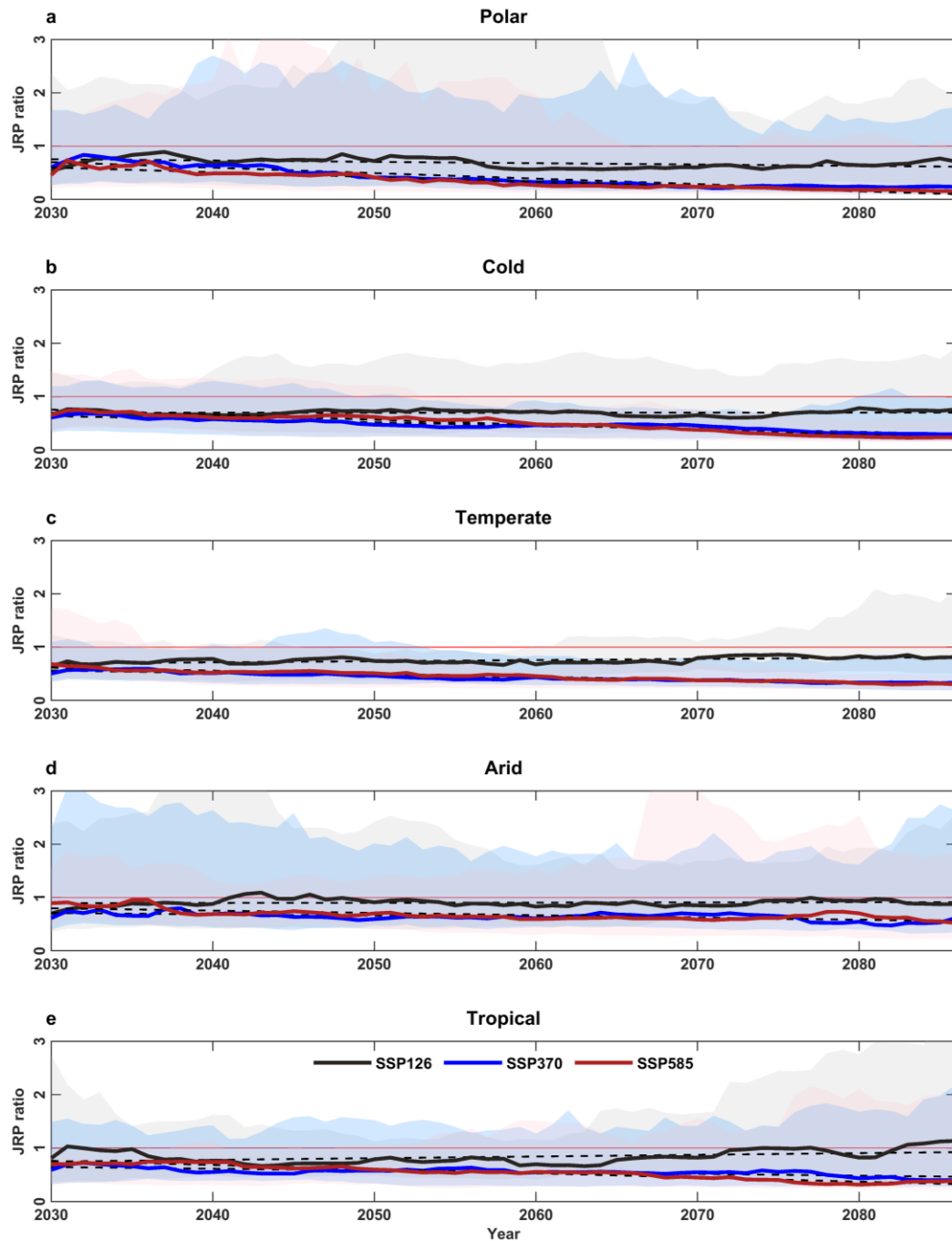


Figure S7 Projected trends and associated uncertainty in JRP ratios of hydrological droughts in the five climate zones. The colored shaded area represents the uncertainty across models (five global climate models multiply by five hydrological models) and the black (colored dashed) line represents the linear trend line (spatially-averaged JRP ratios) of hydrological droughts.

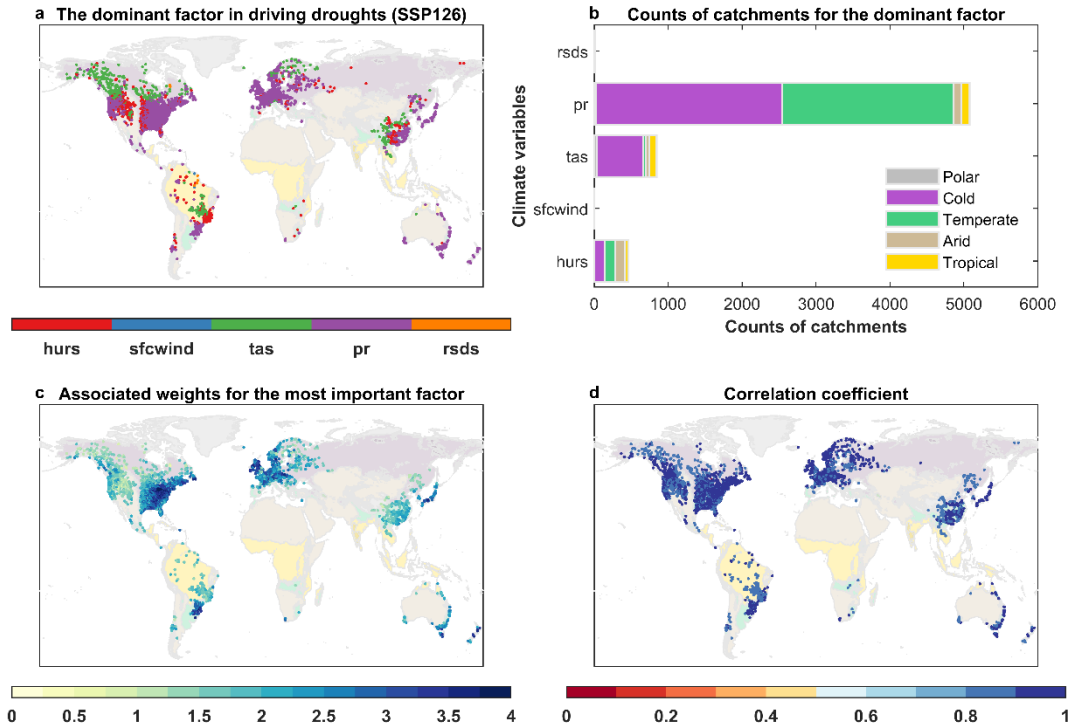


Figure S8 The dominant factor driving future droughts under the SSP126 scenario over catchments in the five climate zones. a, The spatial distribution of the dominant factor. b, Counts of catchments for each dominant factor. c, The spatial distribution of associated weights for the dominant factor in the random forest models. d, Performance of the random forest models (measured by the Pearson correlation coefficient between the calculated and predicted SRI series).

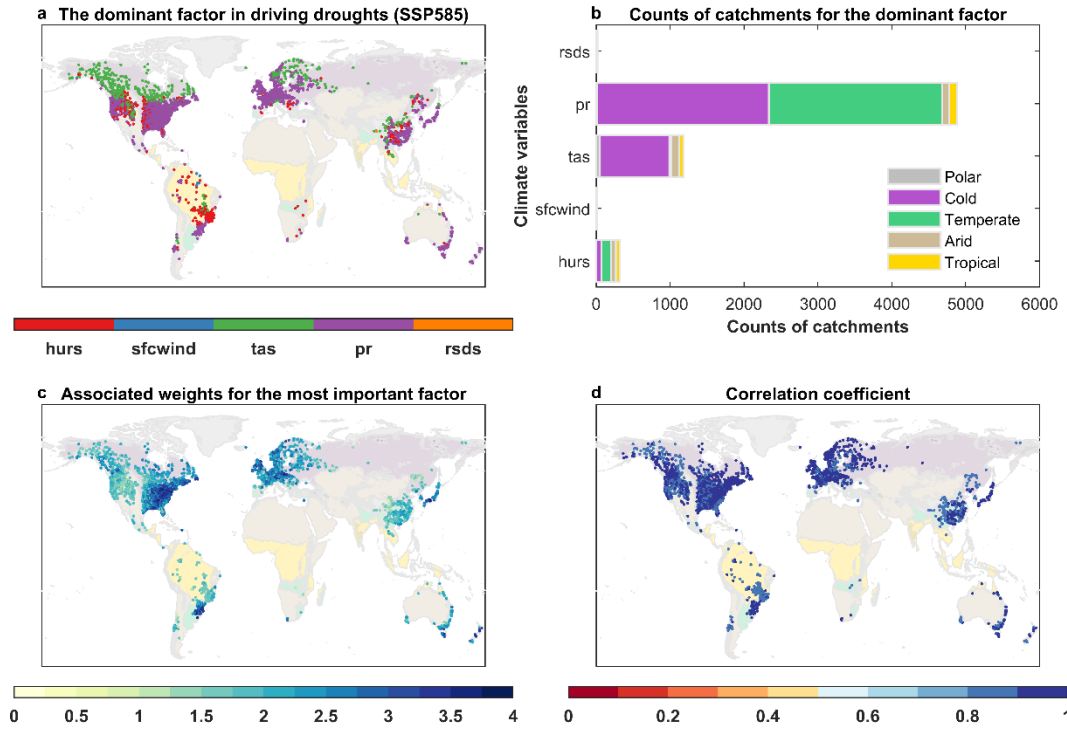


Figure S9 The dominant factor in driving future droughts under the SSP585 scenario over catchments in the five climate zones. a, The spatial distribution of the dominant factor. b, Counts of catchments for each dominant factor. c, The spatial distribution of associated weights for the dominant factor in the random forest models. d, Performance of the random forest models (measured by the Pearson correlation coefficient between the calculated and predicted SRI series).

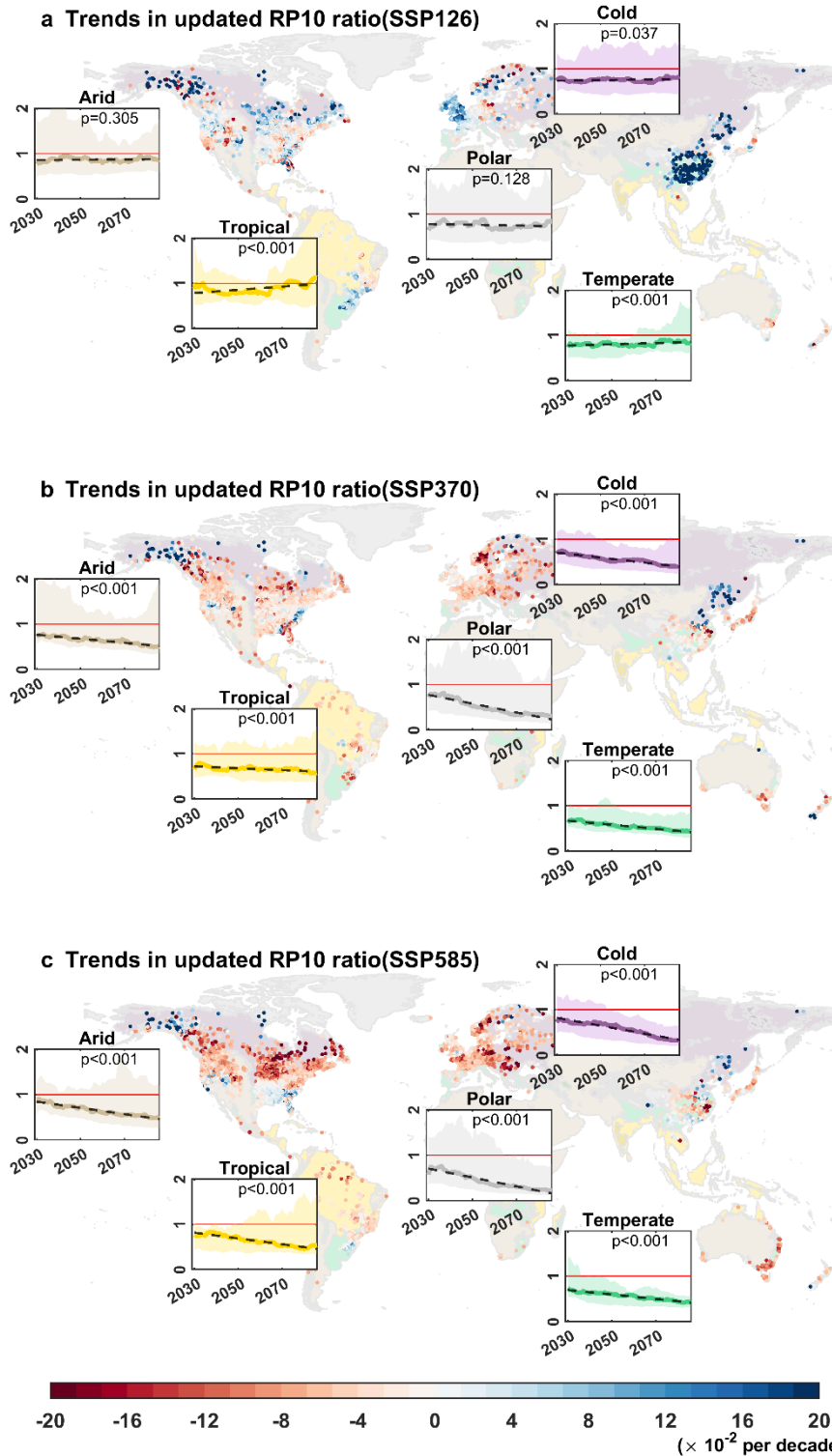


Figure S10 Projected trends in 10-year JRP (RP10) ratios for hydrological droughts. The colored circles denote projected trends in 10-year JRP ratios during the 2015-2100 period (computed for each moving 30-year time window) from MMM results under the SSP126, 370, 585 scenarios, respectively. Decreasing trends indicate decreasing JRP and increasing drought hazards. The colored shaded area on the graphs represents the uncertainty between models and the dark (colored) line represents the linear trend line (spatially averaged 10-year JRP ratios) for hydrological droughts. p -values are statistically significant at the 0.001 confidence level. The x-axes show years and the y-axes show projected frequency ratios.

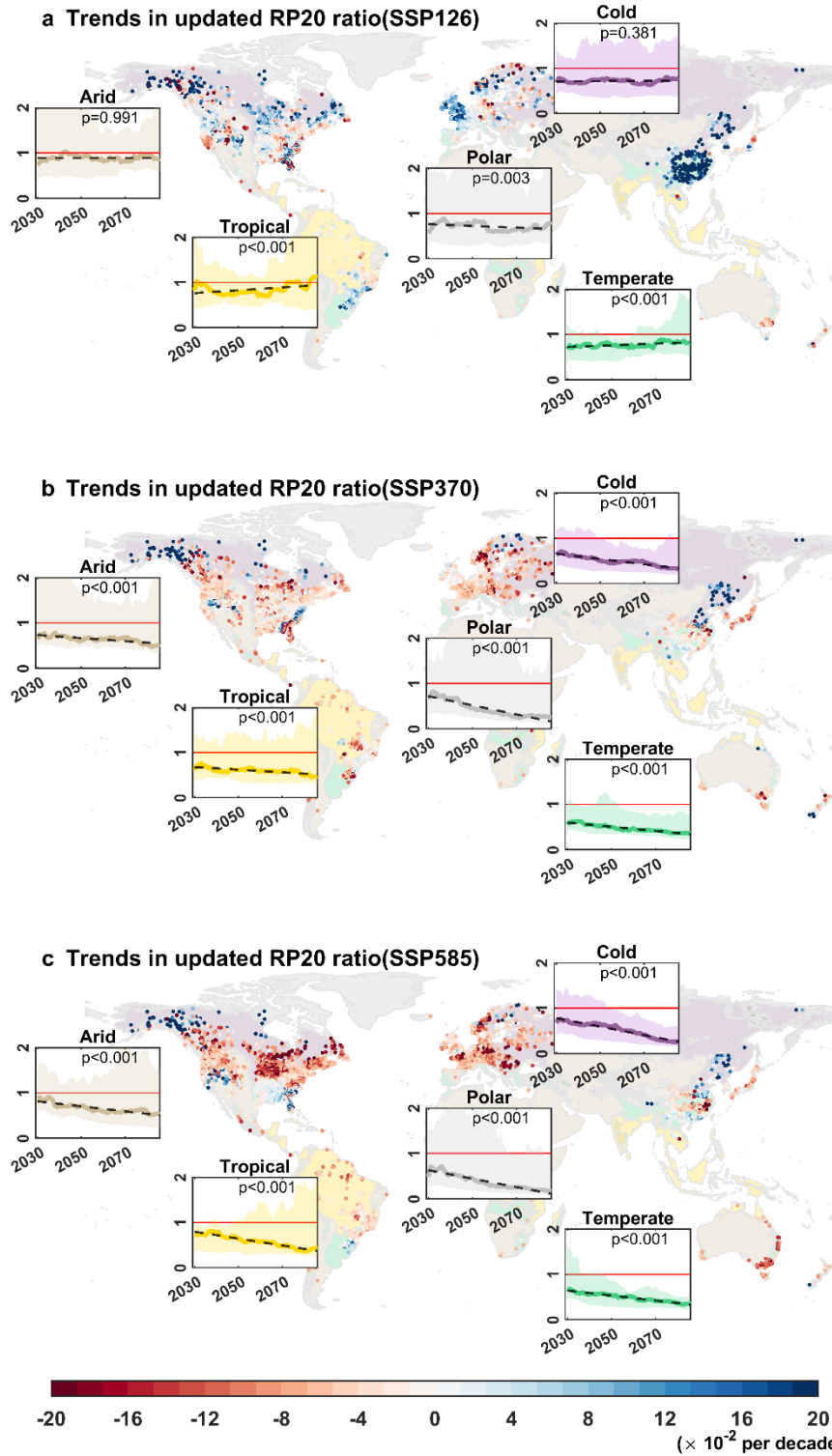


Figure S11 Projected trends in 20-year JRP (RP20) ratios for hydrological droughts. The colored circles denote projected trends in 20-year JRP ratios during the 2015-2100 period (computed for each moving 30-year time window) from MMM results under the SSP126, 370, 585 scenarios, respectively. Decreasing trends indicate decreasing JRP and increasing drought hazards. The colored shaded area on the graphs represents the uncertainty between models and the dark (colored) line represents the linear trend line (spatially averaged 20-year JRP ratios) for hydrological droughts. p -values are statistically significant at the 0.001 confidence level. The x-axes show years and the y-axes show projected frequency ratios.

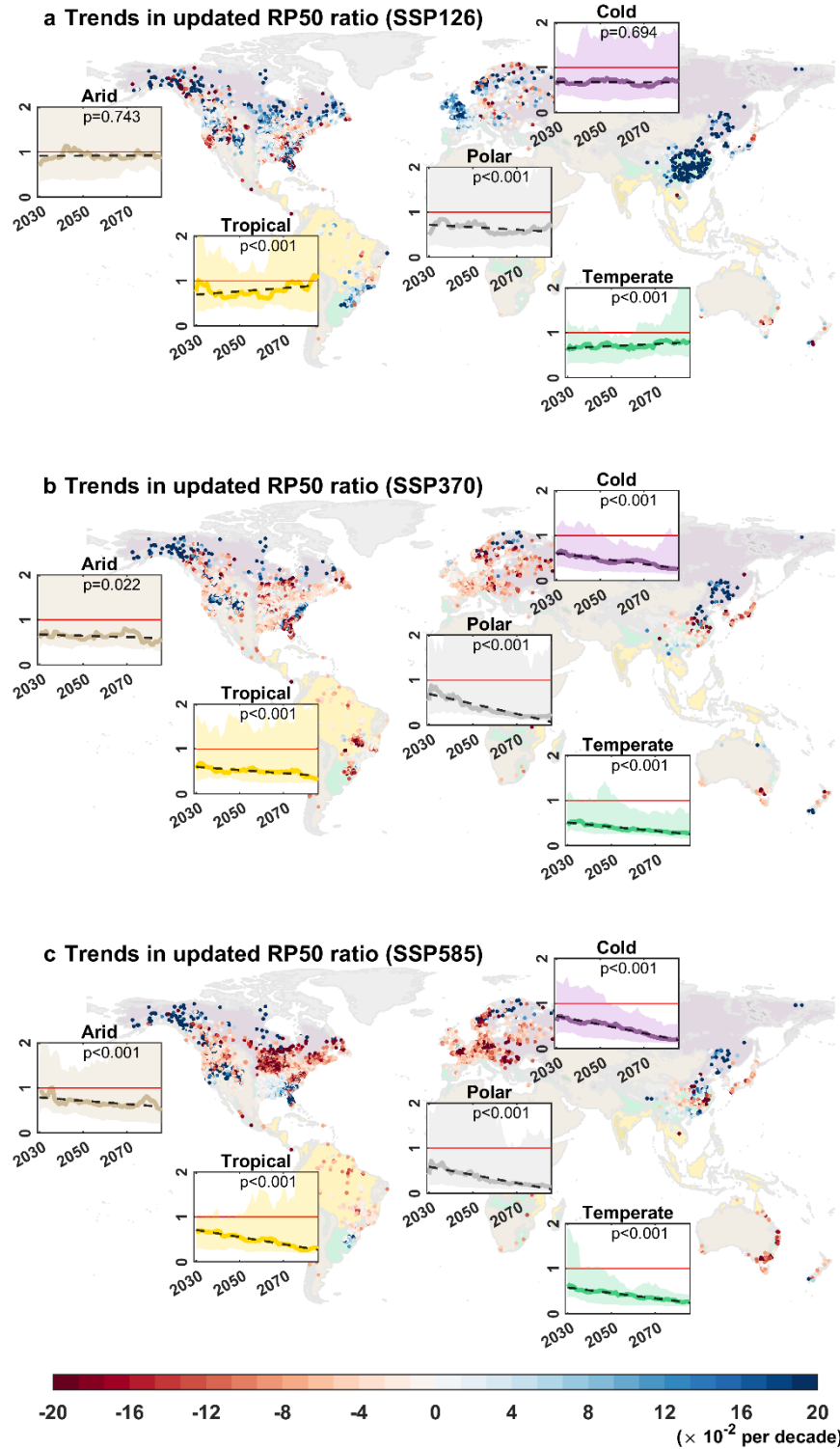


Figure S12 Projected trends in 50-year JRP (RP50) ratios for hydrological droughts. The colored circles denote projected trends in 50-year JRP ratios during the 2015-2100 period (computed for each moving 30-year time window) from MMM results under the SSP126, 370, 585 scenarios, respectively. Decreasing trends indicate decreasing JRP and increasing drought hazards. The colored shaded area on the graphs represents the uncertainty between models and the dark (colored) line represents the linear trend line (spatially averaged 50-year JRP ratios) for hydrological droughts. p -values are statistically significant at the 0.001 confidence level. The x-axes show years and the y-axes show projected frequency ratios.

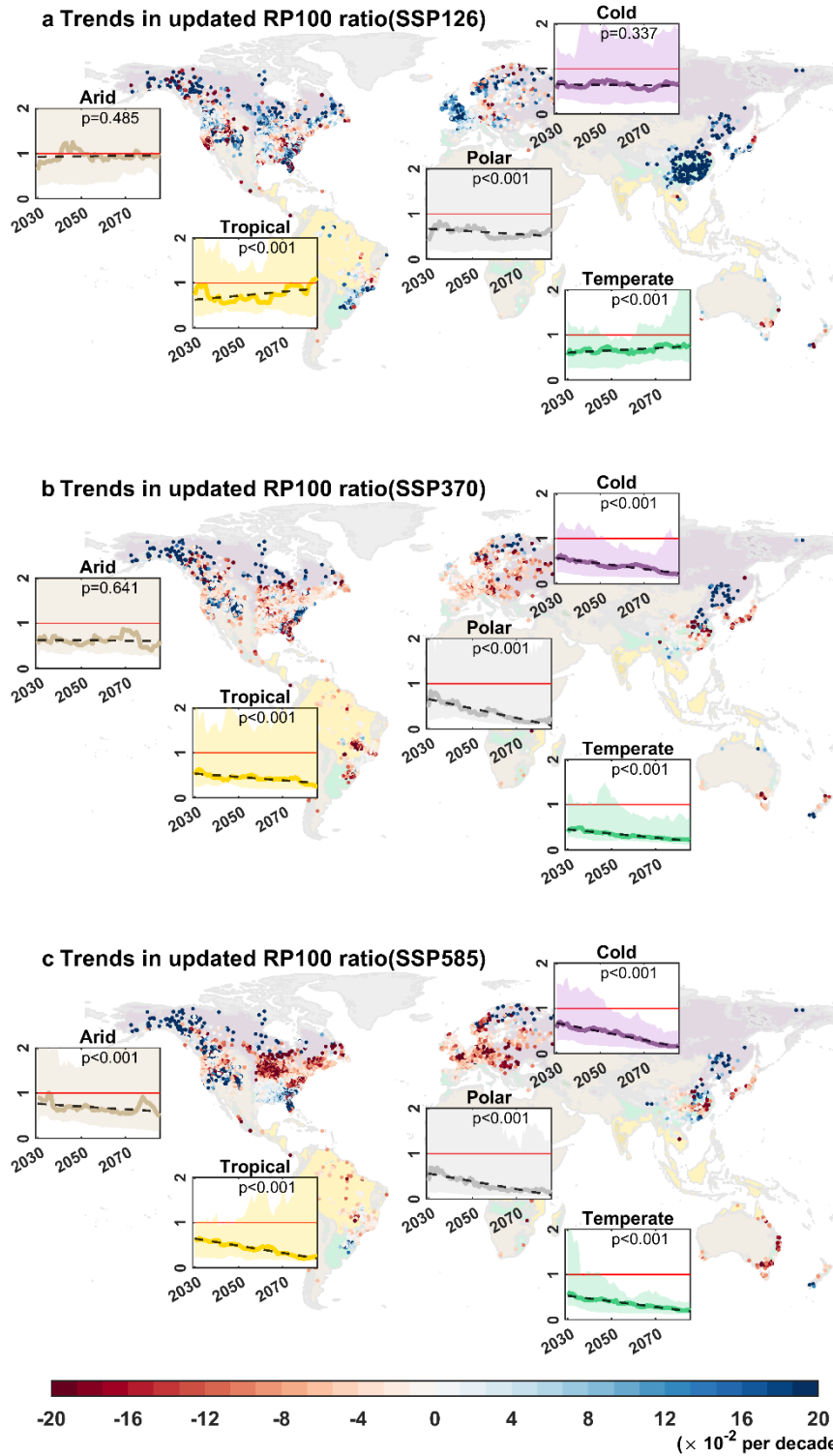


Figure S13 Projected trends in 100-year JRP (RP100) ratios for hydrological droughts. The colored circles denote projected trends in 10-year JRP ratios during the 2015-2100 period (computed for each moving 30-year time window) from MMM results under the SSP126, 370, 585 scenarios, respectively. Decreasing trends indicate decreasing JRP and increasing drought hazards. The colored shaded area on the graphs represents the uncertainty between models and the dark (colored) line represents the linear trend line (spatially averaged 100-year JRP ratios) for hydrological droughts. p -values are statistically significant at the 0.001 confidence level. The x-axes show years and the y-axes show projected frequency ratios.

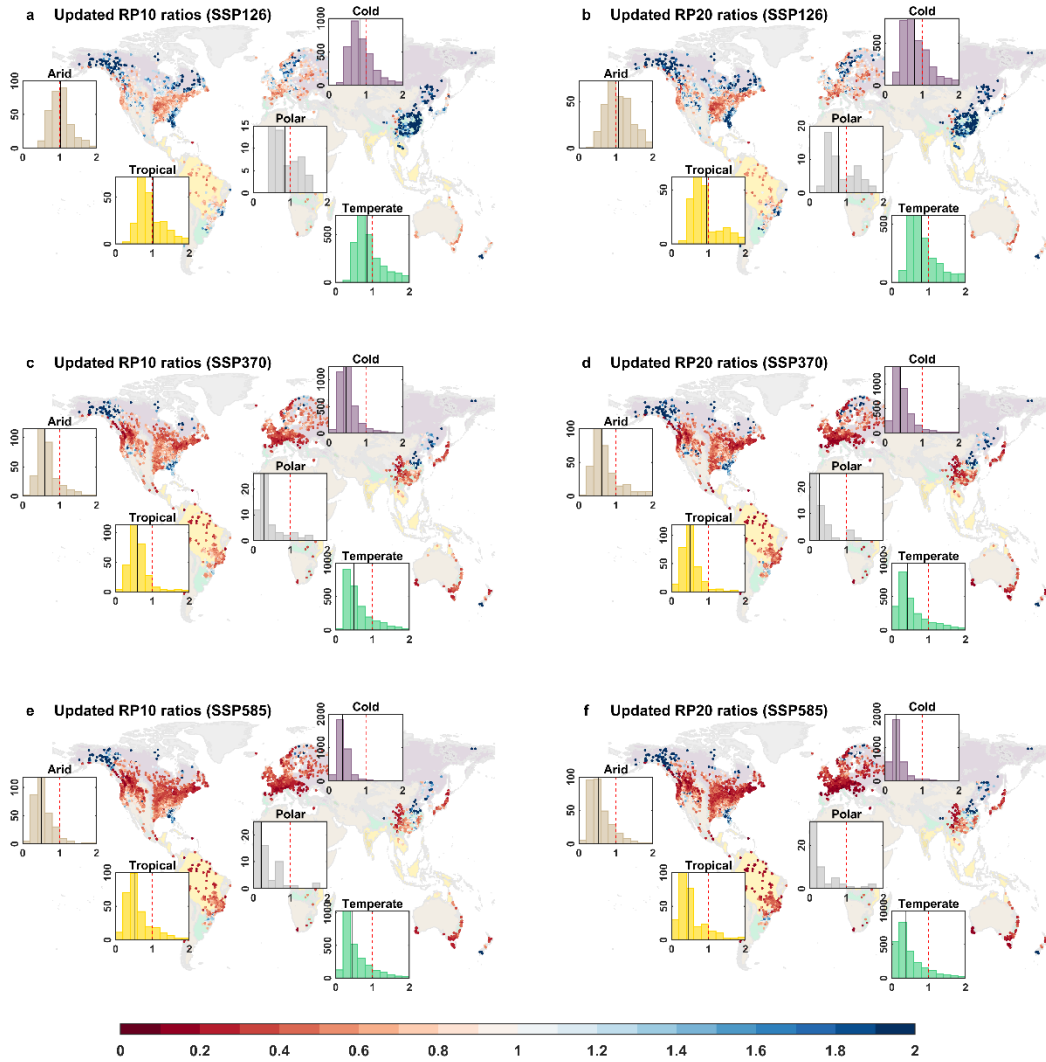


Figure S14 Future changes in RP10 and RP20 ratios by the end of 21st century. a,c,e, Updated 10-year JRP ratios (RP10 ratios) by the 2071-2100 period relative to the 1985-2014 period from MME under the SSP126, 370, 585 scenarios, respectively. The vertical red dashed line denotes 1, indicating unchanged return period; the vertical black line denotes the spatially-averaged value of each climate zone. b,d,f, Updated 20-year JRP ratios (RP20 ratios) by the 2071-2100 period relative to the 1985-2014 period from MME under the SSP126, 370, 585 scenarios, respectively. The vertical red dashed line denotes 1, indicating unchanged return period; the vertical black line denotes the spatially-averaged value of each climate zone.

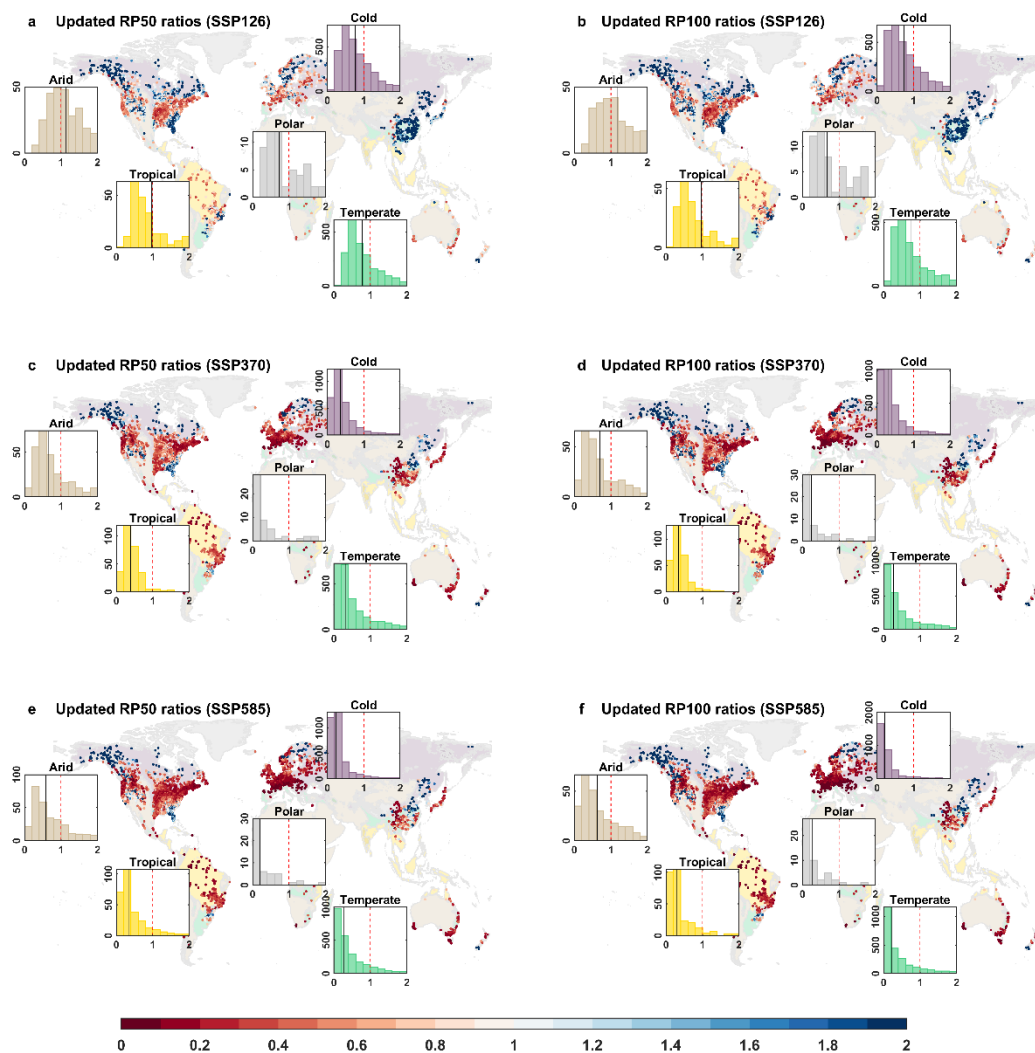


Figure S15 Future changes in RP50 and RP100 ratios by the end of 21st century. a,c,e, Updated 50-year JRP ratios (RP50 ratios) by the 2071-2100 period relative to the 1985-2014 period from MME under the SSP126, 370, 585 scenarios, respectively. The vertical red dashed line denotes 1, indicating unchanged return period; the vertical black line denotes the spatially-averaged value of each climate zone. b,d,f, Updated 100-year JRP ratios (RP100 ratios) by the 2071-2100 period relative to the 1985-2014 period from MME under the SSP126, 370, 585 scenarios, respectively. The vertical red dashed line denotes 1, indicating unchanged return period; the vertical black line denotes the spatially-averaged value of each climate zone.

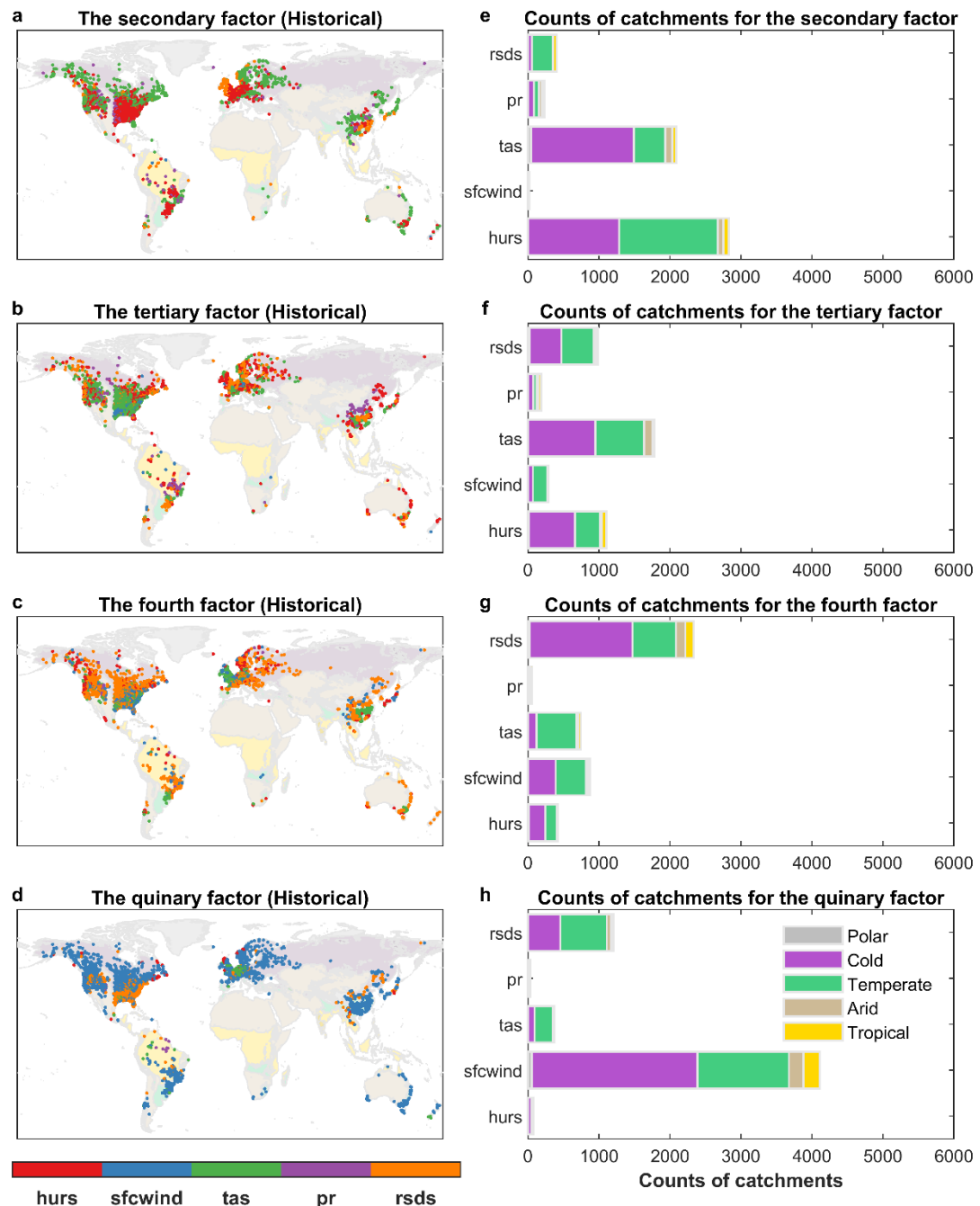


Figure S16 The spatial distribution of driving factors for historical (1985-2014) droughts over catchments in the five climate zones. a,e, The spatial distribution and counts of catchments for the secondary driving factors. b,f, The same as a,e, but for the third driving factors. c,g, The same as a,e, but for the fourth driving factors. d,h, The same as a,e, but for the quinary driving factors.

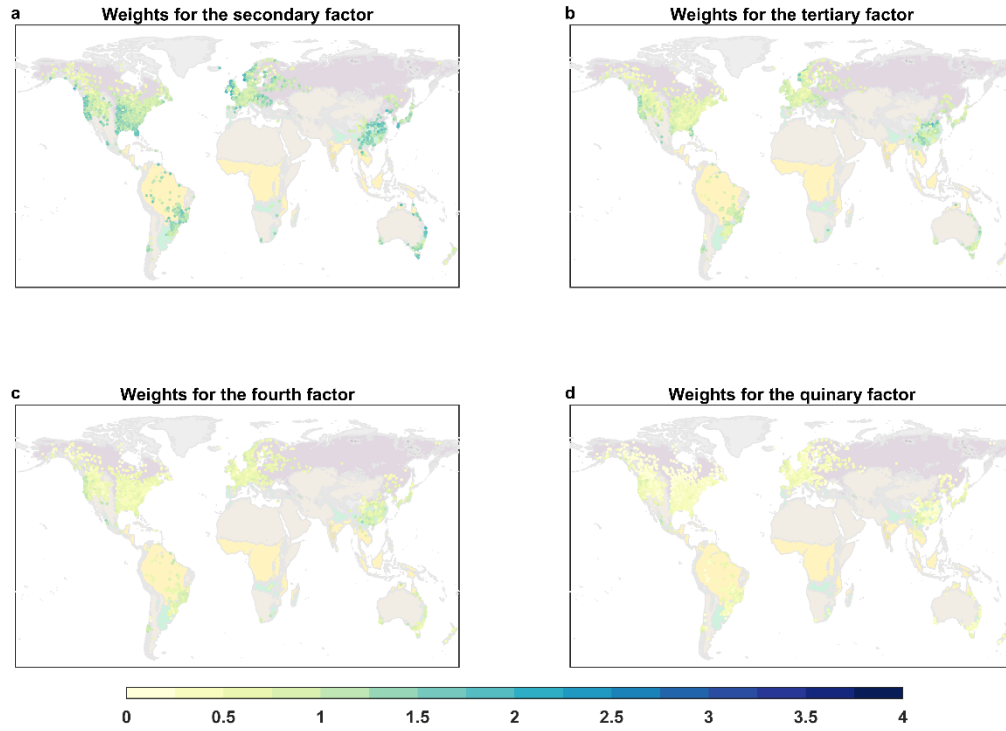


Figure S17 The spatial distribution of weights for the driving factors during the historical (1985-2014) period over catchments in the five climate zones. a, The spatial distribution of weights for the secondary driving factors. b, The spatial distribution of weights for the tertiary driving factors. c, The spatial distribution of weights for the fourth driving factors. d, The spatial distribution of weights for the quinary driving factors.

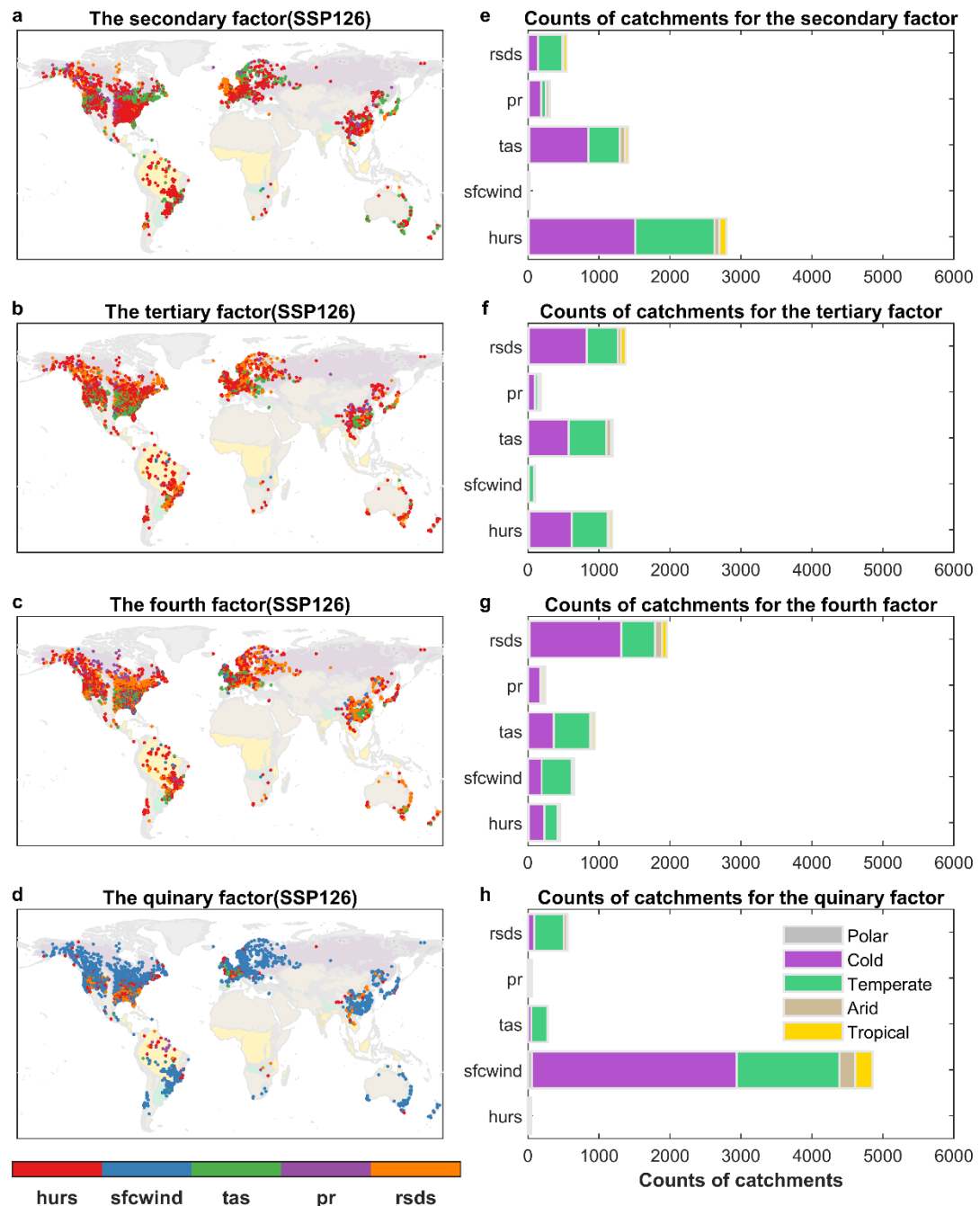


Figure S18 The spatial distribution of driving factors for future (2071-2100) droughts over catchments for five climate zones under SSP126 scenario. a,e, The spatial distribution and counts of catchments for the secondary driving factors. b,f, The same as a,e, but for the tertiary driving factors. c,g, The same as a,e, but for the fourth driving factors. d,h, The same as a,e, but for the quinary driving factors.

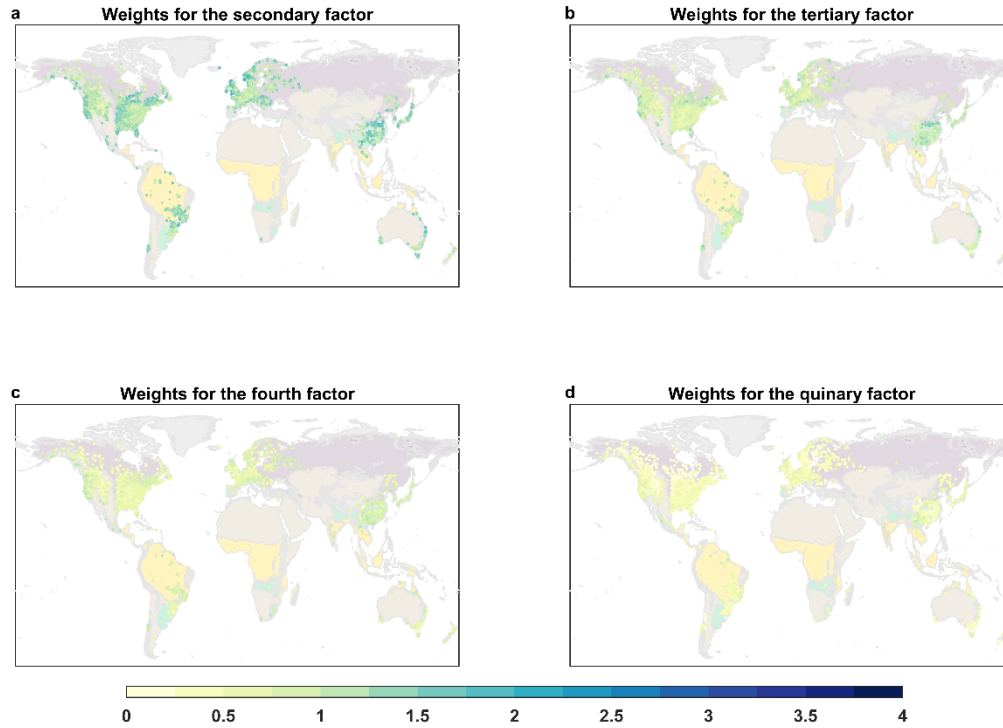


Figure S19 The spatial distribution of weights for the driving factors during future (2071-2100) period over catchments for five climate zones under the SSP126 scenario. a, The spatial distribution of weights for the secondary driving factors. b, The spatial distribution of weights for the tertiary driving factors. c, The spatial distribution of weights for the fourth driving factors. d, The spatial distribution of weights for the quinary driving factors.

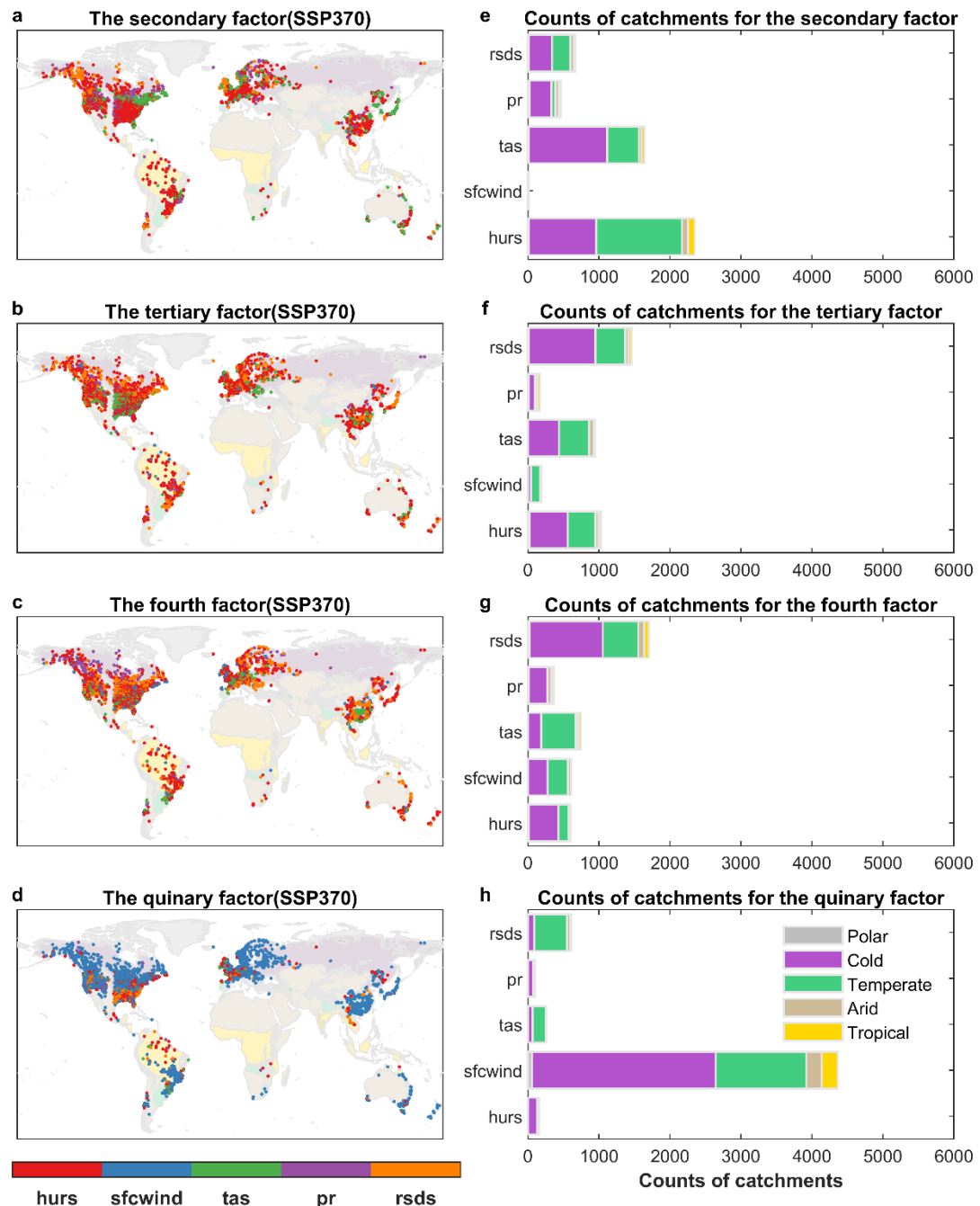


Figure S20 The spatial distribution of driving factors for future (2071-2100) droughts over catchments for five climate zones under SSP370 scenario. a,e, The spatial distribution and counts of catchments for the secondary driving factors. b,f, The same as a,e, but for the tertiary driving factors. c,g, The same as a,e, but for the fourth driving factors. d,h, The same as a,e, but for the quinary driving factors.

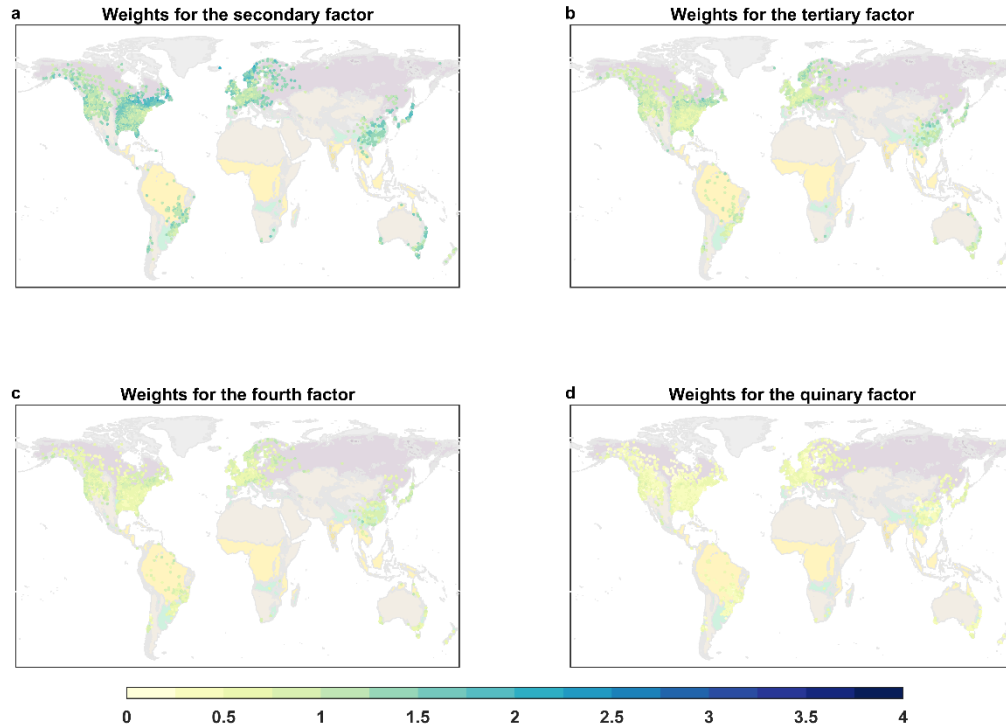


Figure S21 The spatial distribution of weights for the driving factors during future (2071-2100) period over catchments for five climate zones under the SSP370 scenario. a, The spatial distribution of weights for the secondary driving factors. b, The spatial distribution of weights for the tertiary driving factors. c, The spatial distribution of weights for the fourth driving factors. d, The spatial distribution of weights for the quinary driving factors.

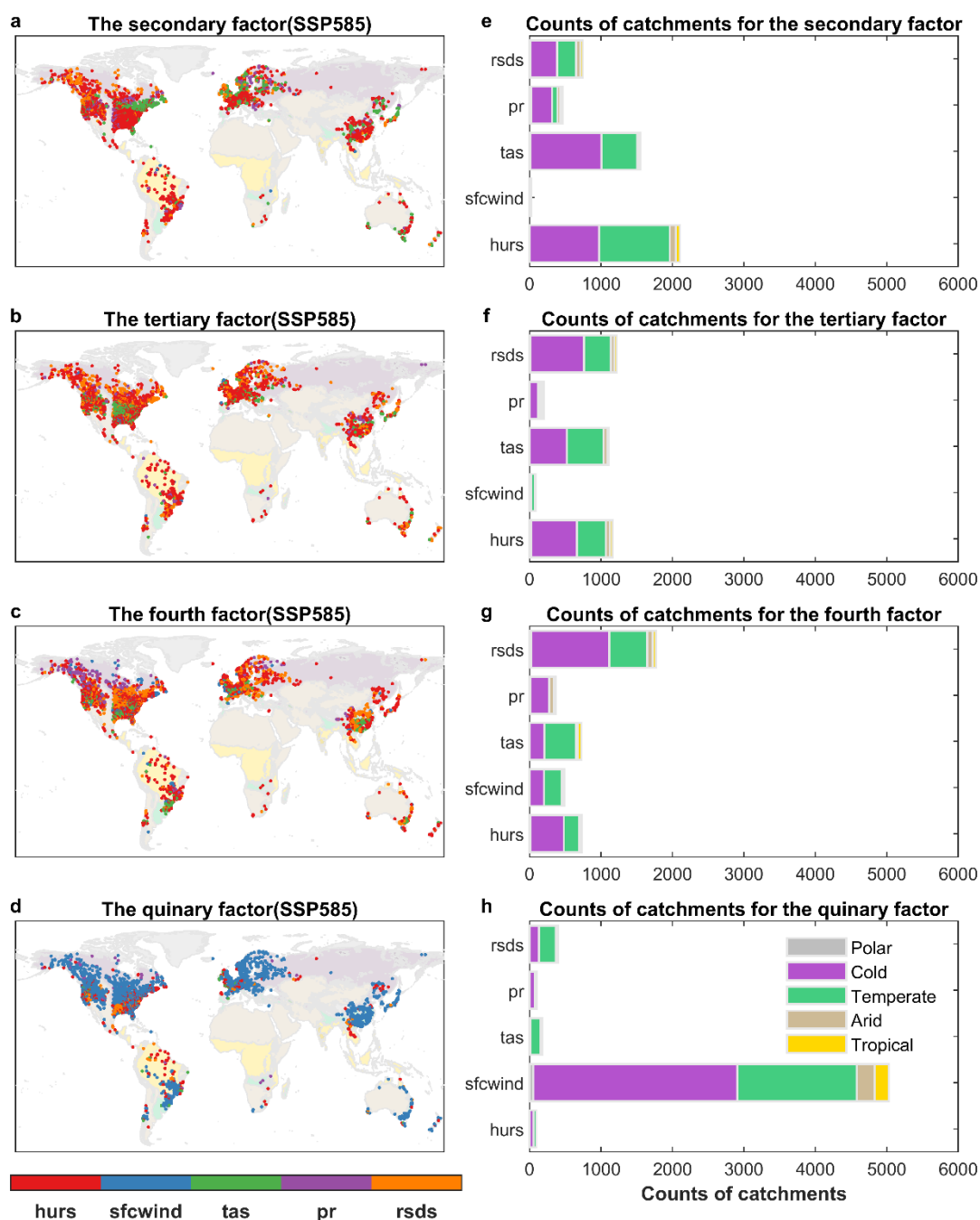


Figure S22 The spatial distribution of driving factors for future (2071-2100) droughts over catchments for five climate zones under SSP585 scenario. a,e, The spatial distribution and counts of catchments for the secondary driving factors. b,f, The same as a,e, but for the tertiary driving factors. c,g, The same as a,e, but for the fourth driving factors. d,h, The same as a,e, but for the quinary driving factors.

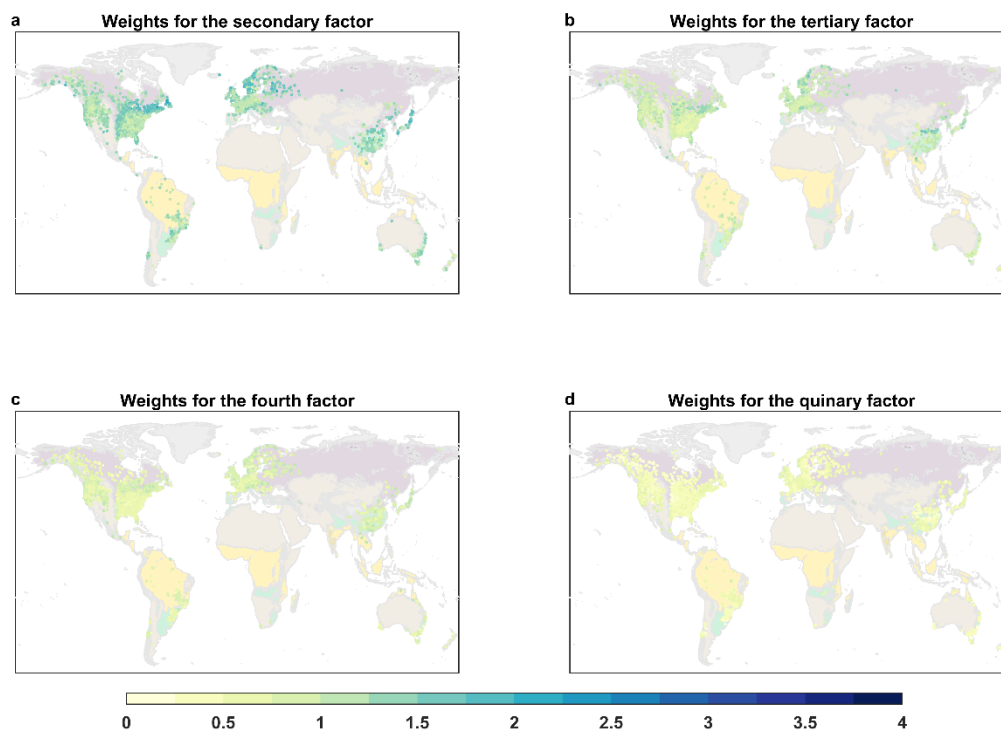


Figure S23 The spatial distribution of weights for the driving factors during future (2071-2100) period over catchments for five climate zones under the SSP585 scenario. a, The spatial distribution of weights for the secondary driving factors. b, The spatial distribution of weights for the tertiary driving factors. c, The spatial distribution of weights for the fourth driving factors. d, The spatial distribution of weights for the quinary driving factors.